Little work has been done in the area of heat transfer within a fluidized bed. It is almost universally assumed that the emulsion-bubble thermal interaction has no effect on the overall performance of the reactor. It is possible, however, to get some semi-empirical expressions by analogy to the mass transfer equations. All of the same mechanisms would be involved. Due to the small size of most bubbles relative to the dimensions of the reactor and the intimate contact of the gas with the solids in the cloud it is not unreasonable to assume that a fluidized bed is isothermal.

Fluidized Bed Model. The model developed to represent the fluidized beds in the staged reactor is based on the bubble assemblege idea first put forward by Kato and Wen. (1969) Figure 15 shows the scheme used to divide the bed into stages and the associated nomenclature. Kato and Wen's basic model was modified to include provisions for local back-flow of gas, the presence of three "phases" as opposed to two, the possibility of reactions in any of these three phases,and the possibility of an uncatalyzed reaction.

In the approach put forth by Kato and Wen, the bed is first divided into a series of compartments. Each compartment has a height that is equal to the average

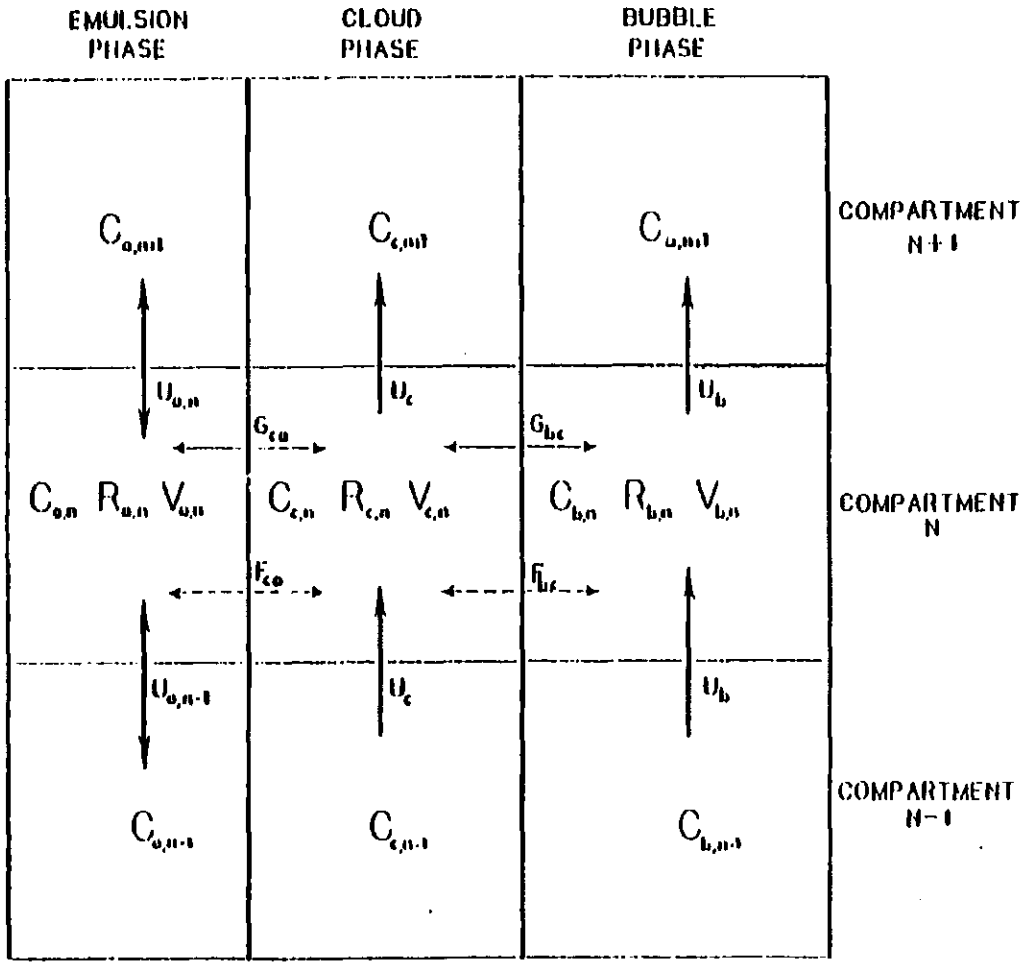

Figure 15. The scheme used to divide the bed for the current model and the associated nomenclature.

bubble diameter at that level in the bed. Thus the compartments higher in the bed are larger than the lower ones. The transport of material is considered for each of the phases in each compartment. Material flowing from one compartment to the next stays in the same phase. Once the species arrive in a given compartment it can either react, diffuse into an adjacent phase, flow into an adjacent phase, or flow into the next compartment. The coefficients associated with each transfer process must be determined empirically.

The equations in Table 1 are derived from material balances around each phase. The determination of the parameters to be used in these equations is the area in which the model is the weakest. The expressions for these parameters are either based on simplifying assumptions or on empirical correlations. In the initial model development stage of the project relations that have been published in the literature will be used.

The first parameters that must be calculated are those that apply to the bed as a whole. These parameters are the expanded bed height and the height of the jetting region. The expanded bed height comes from Peters et al. (1982).

Table 1. The equations used to model a fluidized bed.

Bubble Phase
$\emptyset = U_{BS_{P-1}} AC_{B_{P-1}} - U_{BS_P} AC_{B_P} - G_{BC} AC_{B_P} - F_{BC_P} V_{B_P} (\frac{C_{B_P}}{H} - C_{C_P}) - V_{B_P} R_{V_B}$
Cloud Phase
$\emptyset = U_{CS_{P-1}} AC_{C_{P-1}} - U_{CS_P} AC_{C_P} - G_{CE} AC_{C_P} + G_{BC} AC_{B_P} - F_{CE_P} V_{B_P} (\frac{C_{C_P}}{H} - C_{E_P}) + F_{BC} V_{B_P} (\frac{C_{B_P}}{H} - C_{C_P}) - V_{C_P} R_{V_C}$
Emulsion Phase
Forward Gas Flow
$\emptyset = U_{ES_{P-1}} AC_{E_{P-1}} - U_{ES_P} AC_{E_P} + G_{CE} AC_{C_P} + F_{CE} V_{B_P} (\frac{C_{C_P}}{H} - C_{E_P}) - V_{E_P} R_{V_E}$
First compartment to experience backflow
$\emptyset = U_{ES_P} AC_{E_{P+1}} + U_{ES_{P-1}} AC_{ES_{P-1}} + G_{CE} AC_{C_P} + F_{CE} V_{B_P} (\frac{C_{C_P}}{H} - C_{E_P}) - V_{E_P} R_{V_E}$

Table 1. cont.

Subsequent backflow compartments
$\emptyset = U_{ES_P} AC_{E_{P+1}} - U_{ES_{P-1}} AC_{E_P} + G_{CE} AC_{C_P} + F_{CE} V_{B_P} \left(\frac{C_{C_P}}{H} - C_{E_P}\right) - V_{E_P} R_{V_E}$

$$H = \frac{H_{mf}}{1 - \frac{Y\,(U_o - U_{mf})}{U_o - U_{mf} + 0.71\,(G * D_{BM})^{1/2}}} \qquad (10)$$

H = The expanded bed height.

H_{mf} = The height of the bed just as it is fluidized.

Y = A proportionality constant

U_o = Initial superficial gas velocity

U_{mf} = Minimum superficial gas velocity required to fluidize the bed

G = Gravitantional acceleration

D_{BM} = Maximum stable bubble diameter in the bed

The expression used for the height of the jetting region was suggested by Mori and Wen (1984)

$$H_j = \frac{D_p}{(0.0007 + 0.556 * D_p) * (A/N_D * (U_o - U_{mf})^{0.35}} \qquad (11)$$

H_j = Height of the jetting region

D_p = Diameter of a solid particle

A = Cross-sectional area of the reactor

N_D = Number of orifices in the distributor plate

The velocities of the gas in each of the phases of a given compartment are perhaps the easiest parameters to

obtain. The gas velocity in the bubble phase is simply the linear velocity of the bubbles rising in the bed multiplied by the fraction of the bed occupied by the bubbles

$$U_{BS} = U_B \delta_B \epsilon_B \qquad (12)$$

U_B = linear rise velocity of a bubble

δ_B = volume fraction of the bed occupied by the bubble phase.

ϵ_B = void fraction in bubble phase

Now assuming that the bubble and its associated cloud phase rise at the same velocity an expression for the velocity in the cloud phase can be obtained.

$$U_{CS} = \frac{\delta_C \epsilon_C}{\delta_B \epsilon_B} U_{BS} \qquad (13)$$

δ_C = Volume fraction of bed occupied by the cloud phase.

ϵ_C = Void fraction in cloud phase.

Finally a term for the superficial velocity in the emulsion phase can be derived by assuming that the sum of the superficial velocities in each phase is the overall superficial velocity. Thus

$$U_{ES} = U_{\emptyset} - (U_{BS} + U_{CS}) \qquad (14)$$

$U_{\emptyset}$ = Overall superficial velocity

All that remains to determine is the linear rise velocity of the bubbles. Using a correlation presented by Davidson and Harrison (1982) that is commonly accepted

$$U_B = (U_{\emptyset} - U_{mf}) + 0.71 (G D_B)^{0.5} \qquad (15)$$

U_{mf} = Minimum velocity needed to fluidize the bed.

G = Gravitational acceleration (cm/s)

D_B = Equivalent spherical bubble having the same volume as the actual bubble

Another set of parameters that must be determined is the diffusion transport coefficients. By assuming that the film transport coefficients are small compared to the bulk dispersion Peters et al. (1982) derived an expression for the coefficients

$$F_{BC} = 2.0 (\frac{U_{mf}}{D_B}) \qquad (16)$$

and

$$F_{CE} = 6.78 \left(\frac{D_G \epsilon_{mf} U_B}{D_B} \right)^{0.5} \qquad (17)$$

D_G = Molecular diffusion coefficient

ϵ_{mf} = Bed void fraction when the gas velocity is the minimum velocity needed to fluidize the bed

The final set of parameters of interest are the cross flow velocities. These values are determined from material balance considerations. The difference in the flow from one compartment to the next has be be equal to the net flow out of the phase of interest. Thus

$$P_{BC} = U_{BS_P} - U_{BS_{P-1}} \qquad (18)$$

and

$$P_{CE} = P_{BC} + U_{CS_P} - U_{CS_{P-1}} \qquad (19)$$

The expression to be used to calculate the reaction rate depends on the process under consideration. A separate set of equations exist for each component. These equations are dependant on one another, the concentrations in the previous compartment, and the concentrations in the

next compartment. Due to the nonlinearity produced by the rate expressions it is not possible to obtain an analytic solution to the equation system. An iterative computer technique was used to solve the equations.

Figure 16 shows a flow diagram for the program. Versions of the program were prepared in both FORTRAN and a spread sheet form. The FORTRAN program is listed in Appendix B.

Slurry Reactor

Behavior. Interest in slurry reactors has expanded much more recently than that in fluidized beds. Because of that, there has been considerably fewer studies examining the behavior of this type of reactor. The recent interest in coal gasification has sparked a renewed interest in the Fischer-Tropsch synthesis. Concurrent with the growth in popularity of the Fischer-Tropsch synthesis has been a growth in interest in the use of slurry reactors. These reactors offer several advantages over fluidized beds in conjunction with the synthesis. Thus the reactor model should also include the possibility of using a slurry reactor instead of a fluidized bed to carry out the Fischer-Tropsch synthesis.

Figure 16. A flow diagram for the fluidized bed computer model.

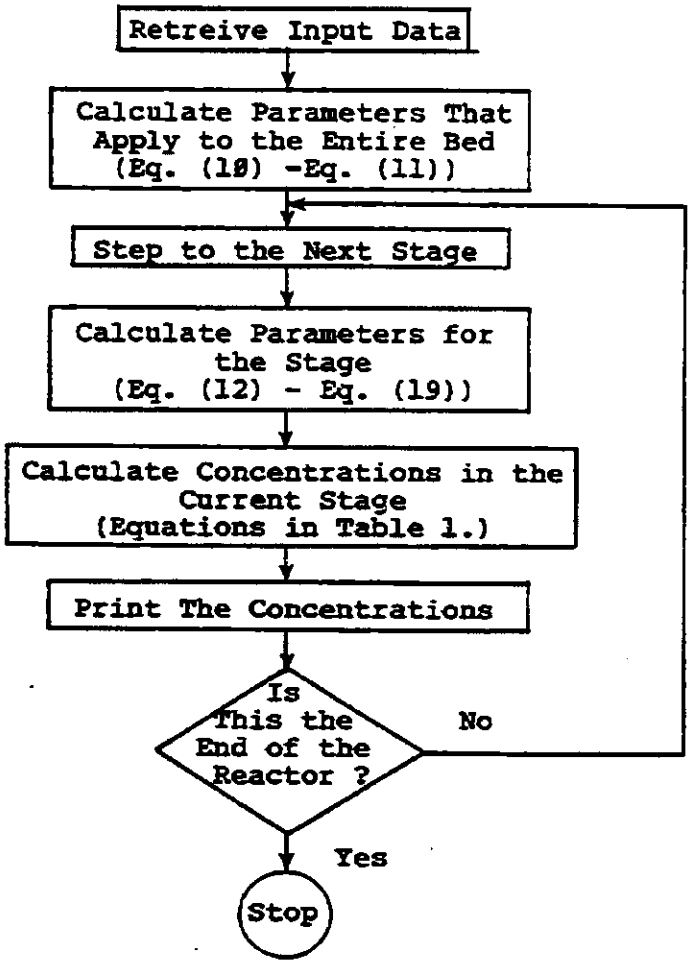

Slurry reactors consist of three actual phases as opposed to the conceptual phases present in fluidized beds. The bulk of the volume of the bed is occupied by a liquid. A gas bubbles up from some type of distributor at the base of the reactor. Solid particles are suspended in the liquid by the mixing action of the bubbles. The bed has no minimum gas flow rate like fluidized beds. There are no major changes in the behavior of the bed until the gas flow rate increases to the point where it causes a foam to form at the top of the liquid.

It is easiest to follow the phenomena occurring in a slurry reactor by tracing the path of the gas through the reactor. As in a fluidized bed, the first component of the reactor encountered is the distributor plate. The distributor design has a very marked effect on the behavior of the bed. The distributor types can be grouped into two classifications. The classes are sintered metal plates and orifices. The sintered plates tend to produce a large number of small bubbles that are all approximately the same size. These bubbles slowly grow as they move up through the bed. Orifice distributors can have as few as one orifice or as many as twenty. Generally they contain less than five orifices. Two types of bubbles are generated by orifice reactors. One type is small and rises slowly through the bed with a swirling motion. The second bubble

type is much larger and tends to rise rapidly with a slug-like motion.

The gases in the bubbles diffuse out into the liquid and eventually reach the surface of the solid particles where the catalyst is located. The gases react then and form the products. Gaseous products diffuse back out to the gas bubbles and are carried out of the reactor while the liquid products remain in the liquid. Thus the slurry liquid of choice is generally the material that is produced by the reaction. This eliminates the need to treat the slurry liquid to remove the reaction products.

If the gas flow is sufficient for the foam to form, the foam starts at the top of the bed. As the flow rate increases, the bottom of the foaming region moves down in the reactor. There is little liquid and virtually no solids in the foam. Thus it is desirable to prevent the foam from forming. Orifice type distributors tend to limit the growth of foam due to the disruptive effects of the large bubbles. Smith et.al. (1984) have produced a good summary of the behavior of slurry reactors.

Previous Modeling. The phenomena occurring in slurry reactors can be broken down into large scale and small scale behavior much like the phenomena occurring in fluidized beds. The small scale phenomena are considerably

simpler in slurry reactors due to the presence of phase barriers that prevent the circulation patterns found in fluidized beds.

Ideal reactors and combinations of ideal reactors can be used to describe the behavior of slurry reactors much like they are used for fluidized bed reactors. These types of models are generally used when the emphasis of the modeling effort is on the kinetics involved. These models have a very limited ability to describe the behavior of reactors other than the one for which they were developed. The most successful ideal reactor models are plug flow reactors. By combining modified reaction rate terms and axial dispersion it is possible to obtain suitable results for most slurry reactors. (Stern et al., 1985a)

Unlike fluidized bed modeling, there has been only one major conceptual approach to modeling slurry reactors. The approach calls for differential equations derived from mass and energy considerations to be solved for both the liquid and gas phase. The first models differed very little from ideal reactor models. Latter treatments have improved the equations by accounting for such phenomena as the change in gas flow due to consumption of reactants, dispersion in the gas phase, heat effects, and nonlinear rate terms. Each successive modification has improved the accuracy of the model at the expense of simplicity. The

equations in the later models are difficult to solve without using some of the most robust numerical techniques available for solving systems of differential equations.

Slurry Reactor Model. The model used to characterize the behavior of the slurry reactor used to carry out the Fischer-Tropsch synthesis is based on the work of Deckwer et. al. (1982) and Stern et. al. (1985) Performing a mass balance for the gas phase at given height we get

$$\emptyset = \frac{d}{dx}\left(D_g \epsilon_g C_g \frac{dy}{dx} \right) - \frac{d}{dx}\left(u_g C_g y \right) - k_l a \left(C_H^* - C_{H,l} \right) \qquad (20)$$

Using the dimensionless units defined in Table 2 the equation becomes

$$\emptyset = \frac{1}{Bo_g} \frac{d^2 y'}{dz^2} - U_g' \frac{d y'}{d z} - St_g \theta \left(y' - x' \right) \qquad (21)$$

the boundary conditions are

$$\left. \frac{d y'}{dz} \right|_{z=1} = \emptyset \qquad (22)$$

$$y'_{z=\emptyset} = 1 \qquad (23)$$

Similarly the equations for the liquid phase are

Table 2. The dimensionless numbers used in the differential equations describing the Fischer-Tropsch reactor.

$x' = x/x_o^*$	(liquid concentration)
$y' = y/y_o$	(gas concentration)
$\theta = T / T_w$	(temperature)
$z = x/H$	(height)
$U_g' = u_g / u_{go}$	(gas velocity)
$Bo_g = \frac{u_{go} H}{D_G \epsilon_G}$	(Bodenstein number)
$Bo_l = \frac{u_{go} H}{D_l \epsilon_l}$	(Bodenstein number)
$St_g = k_l a \frac{L R T_w}{u_{go} He}$	(Stanton number)

Table 2. cont.

$$St_l = k_l a \frac{L}{u_{go}} \quad \text{(Stanton number)}$$

$$St_H = \frac{h\, a_H\, H}{u_{go} \rho\, c_p} \quad \text{(Stanton number)}$$

$$Da = k \epsilon_l H / u_{go} \quad \text{(Damkohler number)}$$

$$\gamma = E_A / R\, T \quad \text{(Arrhenius number)}$$

$$Pe = \frac{u_{go} \tilde{\rho}\, \bar{c}_p\, H}{L\, \lambda_{ax}} \quad \text{(Peclet number)}$$

$$Be = \frac{-\Delta H_R\, P\, y_o}{\tilde{\rho}\, \bar{c}_p\, He\, T_w} \quad \text{(Nameless)}$$

$$\emptyset =$$

$$\epsilon_l D_l \frac{d^2 C_{H,l}}{d z^2} + (k_l a)_H (C_H^* - C_{H,l}) - k_s a_s (C_{H,l} - C_{H,s}) \quad (24)$$

using dimensioned quantities. Assuming

$$k_s a_s (C_{H,l} - C_{H,s}) = r_{H_2} = k \eta_l C_{cat} C_{H,l} \quad (25)$$

and an Arrhenius expression for the rate constant we get in dimensionless units :

$$\emptyset = \frac{1}{Bo_l} \frac{d^2 x'}{dz^2} + St_l (y' - x') - Da \eta C_{cat} e^{-\gamma/\theta_{x'}} \quad (26)$$

The heat balance equation is

$$\emptyset = \epsilon_l \lambda_{ax} \frac{d^2 T}{dx^2} - h a_H (T - T_w) + (-\Delta H_r) r_{H_2} \quad (27)$$

In dimensionless terms we get :

$$\emptyset = \frac{1}{Pe} \frac{d^2 \theta}{dz^2} - St_H (\theta - 1) + Be\ Da \eta C_{cat} e^{-\gamma/\theta_{x'}} \quad (28)$$

using the parameters defined in Table 2. The correlations used to determine the parameters describing the small scale phenomena are listed in Table 3. (Deckwer et al., 1982) The computer program that was developed uses the Crank-Nicholson (Carnahan et al., 1969) method to solve the system of equations. Figure 17 shows the flow diagram of the program. The FORTRAN program itself is listed in Appendix B.

Minor Components

The reactor system contains two components that, though not one of the principle reactors, play significant roles in the behavior of the system. These two components were the scrubber and the combustor.

Combustor. The combustor consists of a fluidized bed. However, unlike the pyrolyzer the reactions occurring in the combustor are of no interest. The heat transfer characteristics of the combustor are the main points of interest. Figure 18 shows the paths by which the combustor can lose heat. Heat transfer to the walls of the reactor was modeled using the correlation developed by Wender and Cooper. (Kunii and Levelspiel, 1977) Heat transfer to the

Table 3. Correlations for small scale phenomena occuring in a slurry bed.

$$He = 2.291 \times 10^{7} \exp(-1.2326+(583/T)) \text{ kPa cm}^3/\text{mol}$$

$$\epsilon_G = 0.053\, u_G'^{1.1}$$

$$a = 4.5\, u_g'^{1.1} \text{ cm}^{-1}$$

$$k_l = 0.1165 \left(\frac{\bar{\rho}}{\bar{\mu}} \exp(-4570 / T) \right)^{1/3} \text{ cm/s}$$

$$h = 0.1 \left(\bar{\rho}\, \bar{c}_p u_g'\right) \left(\frac{u_g'^3\, \bar{\rho}}{g\mu} \left(\frac{\bar{\mu}\, \bar{c}_p}{\lambda} \right)^2 \right)^{-0.25} \text{ J/cm}^2 \text{ s K}$$

$$D_g = 5 \times 10^{-4} \left(u_g'/\epsilon_g\right)^3 d_R^{1.5} \text{ cm}^2/\text{s}$$

$$D_l = 3.676\, u_g'^{0.32} d_R^{1.34} \text{ cm}^2/\text{s}$$

$$\lambda_{ax} = D_l\, \bar{\rho}\, \bar{c}_p \text{ J/cm s K}$$